

# Preparation and Characterization of Nano Ferrites

Nisha<sup>1</sup> and Diksha Thakur<sup>2</sup>

<sup>1</sup>Department of Applied Sciences, Chandigarh Group of Colleges, Jhanjeri, Mohali-140307, Punjab, India

<sup>2</sup>Department of Agriculture, Chandigarh School of Business, Jhanjeri, Mohali-140307, Punjab, India

**Abstract:** Nickel ferrite ( $\text{NiFe}_2\text{O}_4$ ) and manganese ferrite ( $\text{MnFe}_2\text{O}_4$ ) had been prepared thru a gentle mechano-chemical route from mixture of (1)  $\text{Ni}(\text{OH})_2$  and  $\alpha\text{-Fe}_2\text{O}_3$  and (2)  $\text{Mn}(\text{OH})_2$  and  $\alpha\text{-Fe}_2\text{O}_3$  powders in a planetary ball mill. The aggregate became activated for various duration. easy mechanochemical response primary to formation of the  $\text{NiFe}_2\text{O}_4$  and  $\text{MnFe}_2\text{O}_4$  spinel stages had been followed with the aid of using the use of X-ray diffraction, Raman and infrared spectroscopy, scanning and transmission microscopy. The spinel segment formation modified into rst discovered after four h of milling (case 1) and after three h (case 2) and its formation modified into completed after 25 h in each times. The synthesized  $\text{NiFe}_2\text{O}_4$  and  $\text{MnFe}_2\text{O}_4$  ferrites have a nanocrystalline shape with crystallite duration of about 30 and 40 nm for times (1) and (2), respectively. There are 5 Raman and 4 IR energetic modes. as a way to apprehend higher the whole device of segment formation, the Mossbauer measurements had been performed.

p.c.: seventy 5.20.-g, 80 one.07.Wx, 81.20.Ev, seventy 4.25.nd

## Introduction

Magnetic nano crystals and nano sized ferrites had been attracting large hobby because of their massive applications, collectively with magnetic memory [1], MRI evaluation retailers [2], e consumer hyperthermia for most cancers therapy [3, 4] and catalysts [5], etc. amongst the ones magnetic materials, spinal-kind ferrite nanoparticles,  $\text{MFe}_2\text{O}_4$  ( $\text{M} = \text{Mn, Co, Ni, Zn, Mg, Fe,}$  and so on.), have received extraordinary interest within the beyond few years because of their suited electromagnetic overall performance and their applications in information garage, medical diagnosis era, sensor era, and magnetic warming and cooling generation [6]. The structural additives of spinel-kind ferrites may be writ- ten as  $(\text{M}^{2+} \text{Fe}^{3+})[\text{M}^{2+}\text{Fe}^{3+}]_2\text{O}_4$ , in which parentheses and rectangular  $1-\lambda$   $\lambda$   $2-\lambda$  internet webweb sites of tetrahedral (A) and octahedral (B) coordination, respectively.  $\lambda$ , this is decided through the guidance process, represents the so-called diploma of inversion described because the fraction of the(A) web sites occupied through  $\text{Fe}^{3+}$  cations [7].  $\text{NiFe}_2\text{O}_4$  and  $\text{MnFe}_2\text{O}_4$  ferrites had been synthesized with the aid of using the use of severa techniques which incorporates strong-state response, co-precipitation, high-temperature self-propagating, microemulsion, solvothermal, mechano synthesis, hydrothermal, sol gel and combustion techniques [8 15]. in this paper, we gift the formation of spinel fer- ceremony segment thru mild mechanochemical treatment [16], starting from special mixtures of powders. The times had been: (1) milling of powders mixture of  $\text{Ni}(\text{OH})_2 + \alpha\text{-Fe}_2\text{O}_3$  throughout 4 25 h and (2) milling of mixture of  $\text{Mn}(\text{OH})_2 + \alpha\text{-Fe}_2\text{O}_3$  for the duration of three 25 h. The Raman and IR spectroscopy in addition to the X-ray diffraction, scanning electron microscopy, transmission electron microscopy and Mossbauer spectroscopy measurements had been used to have a examine the samples mechanochemically handled for special milling times.

## Experimental

The following crystalline powders have been used as beginning materials: (1) nickel (II)-hydroxide ( $\text{Ni}(\text{OH})_2$ , Merck 90 5% purity) and hematite ( $\alpha\text{-Fe}_2\text{O}_3$ , Merck ninety nine% purity) and (2) manganese(II)-hydroxide ( $\text{Mn}(\text{OH})_2$ , Merck 95% purity) and hematite ( $\alpha\text{-Fe}_2\text{O}_3$ , Merck ninety nine% purity). soft mechanochemical synthesis come to be finished in air surroundings in planetary ball mill (Fritsch Pulverisette 5). All samples,

with distinctive beginning compositions and milling instances, have been prepared and milled one after the other. on the expiration of the chosen milling instances (4, 10 and 25 h for the (1) case and 3, 12 and 25 h for (2) case) the mill have become stopped and a small quantity of powder turned into removed from the vial for exam.

Characterization of the obtained samples became performed with the useful resource of:

X-ray diffraction (XRD) assessment of powders handled for diverse intervals of milling instances through manner of a Philips PW 1050 diffractometer prepared with a PW 1730 genera- tor (forty kV 20 mA) the use of Ni filtered Cu  $\alpha$  radiation at the room temperature. Measurements have been performed in  $2\theta$  kind of  $10^\circ$  to  $80^\circ$  with scanning step width of  $0.05^\circ$  and 10 s scanning time in line with step. After XRD measurements, the powder turned into positioned once more in a vial to reap the equal grinding conditions (balls to powder weight ratio).

The Raman measurements of aggregate powders have been achieved the use of Jobin-Ivon T64000 monochromator. An optical microscope with a hundred targets come to be used to focus the 514 nm radiation from a Coherent Innova ninety nine Ar+ laser on the sample. The equal microscope turned into used to build up the backscattered radiation. The scattering moderate dispersed turned into detected through manner of a fee-coupled device (CCD) detection gadget. Room temperature Raman spectra are in spectral variety from one hundred to  $800\text{ cm}^{-1}$ . The not unusualplace power density on the sample modified into  $20\text{ mW mm}^{-2}$

The infrared (IR) measurements have been finished with a BOMEM DA-8 FIR spectrometer. A DTGS pyroelectric detector became used to cowl the wave range variety from 50 to seven hundred  $\text{cm}^{-1}$ .

The morphology of powders and the size of mild mechano-synthesized ferrite crystallites have been tested thru scanning electron microscopy (SEM, model TESCAN Vega TS130MM) and transmission electron microscopy (2 hundred kV TEM, version JEM-2100 UHR, Jeol Inc., Tokyo, Japan).

The Mossbauer spectra of powder samples have been measured at room temperature (RT) the usage of a deliver of  $^{57}\text{Co}$  in Rh ( $1.80\text{ GBq}$ ). The experiments have been finished in wellknown transmission geometry with consistent acceleration calibrated with the useful resource of the laser spectrum. The data have been analyzed via The Win Normos net web page program [17]. Sample thickness correction became performed through the use of transmission essential.

### Results and discussion

Clean mechanochemical synthesis and mechanical milling of (1)  $\text{Ni(OH)}_2 + \text{Fe}_2\text{O}_3 \rightarrow \text{NiFe}_2\text{O}_4 + \text{H}_2\text{O}$  and (2)  $\text{Mn(OH)}_2 + \text{Fe}_2\text{O}_3 \rightarrow \text{MnFe}_2\text{O}_4 + \text{H}_2\text{O}$  modified into moreover finished underneath air surroundings. discern 1a indicates the X-ray diffraction varieties of stoichiometric combos of powdered reactants  $\text{Ni(OH)}_2$  and  $\alpha\text{-Fe}_2\text{O}_3$  in a ball mill for distinctive instances (4, 10, and 25 h). The XRD pat- tern of the start powder is characterised with the useful resource of diffraction peaks just like crystalline  $\text{Ni(OH)}_2$  (JCPDS card seventy 4-2075), NiO (JCPDS card 89-5881),  $\text{NiOOH}$  (JCPDS card 27-0956),  $\alpha\text{-Fe}_2\text{O}_3$  (JCPDS card 89-8104),  $\text{FeO(OH)}$  (JCPDS card 89-6096) and  $\text{NiFe}_2\text{O}_4$  (JCPDS card 89-4927). it could be observed that the number one peaks for the hematite section at  $2\theta = 35.6^\circ$  and  $33.15^\circ$  have been constantly decreased through manner of developing the milling time (Fig. 1a). you could sincerely look at barely wider  $\alpha\text{-Fe}_2\text{O}_3$  peaks of decrease intensity and nearly disappearing  $\text{Ni(OH)}_2$  peaks. it's miles important to observe that in the milling of powder combos among 4 and 10 h takes region a section  $\text{FeO(OH)}$  (JCPDS card 89-6096) and NiO (JCPDS card 89-5881) too. the precept motive for this phenomenon is due to the fact powder  $\text{Fe}_2\text{O}_3$  in an surroundings moist and heated through the use of in- tensive milling reacts with water and  $\text{Ni(OH)}_2$  rapid decomposes thru  $\text{Ni(OH)}_2 \rightarrow \text{NiO} + \text{H}_2\text{O}$ , simply so after 4 h of milling (Fig. 1a) there are a negligible wide variety of peaks just like the start compound  $\text{Ni(OH)}_2$ . in addition, milling up to twenty-five h effects in entire synthesis of new section. all of the diffraction peaks ( $18.4^\circ$ ,  $30.1^\circ$ ,  $35.6^\circ$ ,  $37.3^\circ$ ,  $40\text{ three}.4^\circ$ ,  $50\text{ seven}.4^\circ$  and  $60\text{ two}.8^\circ$ ) of the sample for 25 h of milling time are nicely indexed as cubic spinel section with the fcc shape (fcc face cubic focused). The diffractogram indicates distinctive mirrored image planes listed as (ok h l) (111), (220), (311), (222), (4 hundred), (511) and (440), which shows the spinel.

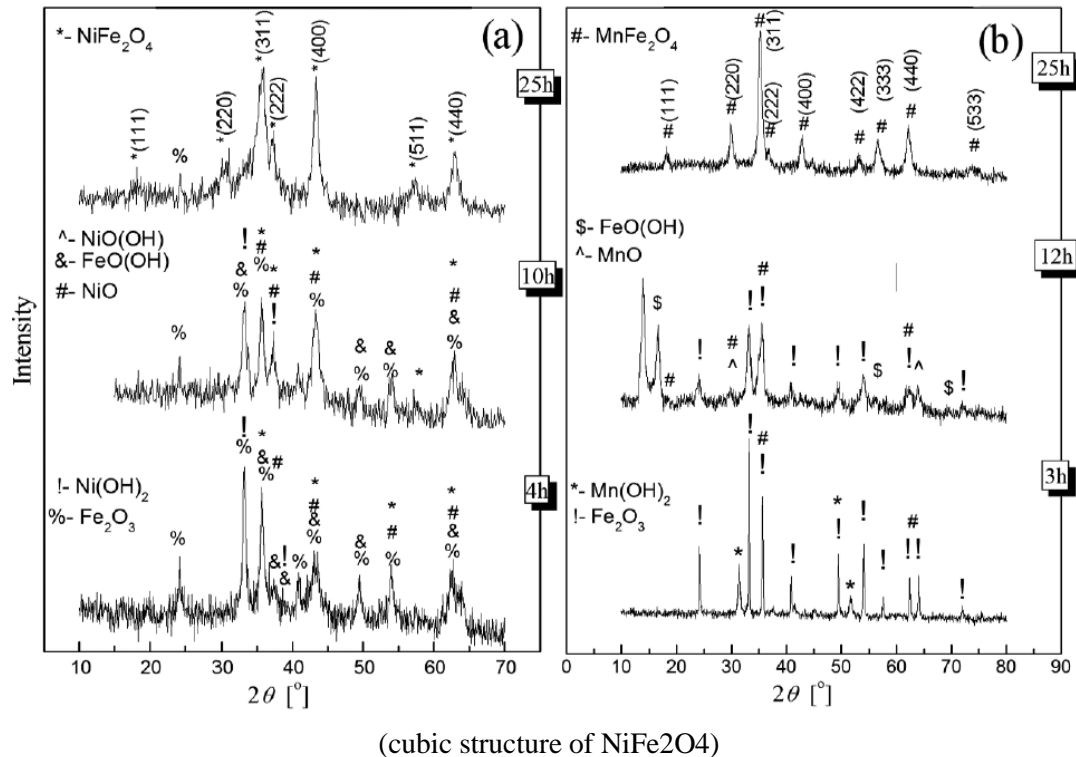


Fig. 1. X-ray diffraction sample of the mixture of Ni(OH)<sub>2</sub> and  $\alpha$ -Fe<sub>2</sub>O<sub>3</sub> and (b) Mn(OH)<sub>2</sub> and  $\alpha$ -Fe<sub>2</sub>O<sub>3</sub> powders after several milling instances.

discern 1b indicates the X-ray diffraction types of combination of Mn(OH)<sub>2</sub> and  $\alpha$ -Fe<sub>2</sub>O<sub>3</sub> powders mechanochemically activated for special milling times (3, 12, and 25 h). The XRD sample of the beginning powder is characterised with the aid of using the usage of sharp diffraction peaks similar to crystalline Mn(OH)<sub>2</sub> (JCPDS card seventy 3-1133) and  $\alpha$ -Fe<sub>2</sub>O<sub>3</sub> (JCPDS card 89-8103) [19]. With growing milling time, the diffraction peaks similar to the clean oxide and hydroxide regularly disappear. all the feature peaks of Mn(OH)<sub>2</sub> and  $\alpha$ -Fe<sub>2</sub>O<sub>3</sub> are well suggested in the spectrum (Fig. 1b). During mechanochemical treatment (3 h) first-rate sharp peaks from the well-crystallized Mn(OH)<sub>2</sub> and  $\alpha$ -Fe<sub>2</sub>O<sub>3</sub> are gift in the XRD sample. the brand new ranges of FeO(OH) (JCPDS card 89-6096) and MnO (JCPDS card seventy 5-1090) arise at a few degree withinside the milling of powder combos amongst 3 and 12 h. it is recognized that the milling method results in overheating of the vessel, and at temperatures higher than 100 °C to the evolution of water vapor. Beginning the sphere results in partial evaporation of water. It might be mentioned that the hydroxides remodel into oxides. on the identical time, there can be found the peaks characteristic of the hydroxide and oxide (Fig. 1b). this may be a end result of beginning of the milling vessel. The motive is almost the same for the samples acquired from the mixture of powders for 12 h of milling time. which means that there may be no further milling as much as 12 h which ends up in complete synthesis of new phase. the appearance of the new peak at  $2\theta = 18.09^\circ, 29.89^\circ, 35.37^\circ, 40 \text{ two}.85^\circ, \text{ fifty } 3.11^\circ, \text{ fifty six}.76^\circ, \text{ sixty two}.13^\circ$  and  $70.37^\circ$ , clearly indicates the formation of the brand new phase of MnFe<sub>2</sub>O<sub>4</sub> (JCPDS card seventy 4-2403) (Fig. 1b). The peaks are nicely listed to the crystal plane of spinel ferrite (adequate h l). (111), (220), (311), (4 hundred), (333), (440) and (533), respectively.

This confirms that the mechanochemical synthesis of MnFe<sub>2</sub>O<sub>4</sub> is feasible and complete for 25 h milling time. the total width at half of maximum of the XRD peaks have become used to calculate the crystallite length D of NiFe<sub>2</sub>O<sub>4</sub> and MnFe<sub>2</sub>O<sub>4</sub> powders the usage of Scherrer's relation [20]:  $D = 0.9\lambda/(\beta \cos \theta)$ , wherein D is the crystallite grain length,  $\lambda = 1.5406$  is the wavelength of the Cu okay $\alpha$ ,  $\beta$  is the broadening of the diffraction line measured at 1/2 of maximum depth (radians). The ensuing fee of the crystallite length, acquired from the (311) maximum effective reflections, are 30 nm for NiFe<sub>2</sub>O<sub>4</sub> and 40 nm for MnFe<sub>2</sub>O<sub>4</sub>, respectively. XRD is the most beneficial evaluation technique for figuring out the crystalline form of substances. but, the XRD of nanocrystalline substances does not offer enough depth of diffraction peaks

important to determine the entire crystallographic facts. extra methods, just like the Raman and IR evaluation, are required to acquire the form evaluation of nanocrystalline materials if you want to distinguish  $MFe_2O_4$  ( $M = Mn, Co, Ni, Cu, Zn, Mg, Cd$ , and plenty of others.) from  $Fe_3O_4$  or  $\gamma-Fe_2O_3$  (feasible impurity ranges) with comparable shape elements and consequently comparable XRD styles.

The crystal shape of  $M_2+Fe_3+O_2-(M_2+ = Mn \text{ or } Ni)$  is spinel (location group  $Fd3m$ ) wherein the lattice of  $O_2^-$  ions office work tetrahedral (A-internet webweb sites) and octahedral (B-internet webweb sites) nearby symmetry. In normal spinel shape, di-valent  $M_2+$  ions handiest occupy A websites, and trivalent  $Fe_3+$  ions occupy B webweb sites. In inverse spinel shape, divalent ions occupy half of of B websites, and trivalent ions occupy the relaxation of B internet webweb sites and all A internet webweb sites. group concept predicts 5 Raman active modes in spinel shape:  $A_{1g} + E_g + 3F_{2g}$  and 4  $F_{1u}$  infrared lively.

$NiFe_2O_4$  has (withinside the main) inverse spinel form. All 5 Raman peaks in  $NiFe_2O_4$  are asymmetric, with shoulder on the low strength side. every peak may be supplied like a doublet. more peaks are associated with the presence of non-identical atoms at the B-internet webweb sites (but with structural ordering over B-internet webweb sites). At a microscopic diploma the form of  $NiFe_2O_4$  can be considered as a mixture of sublattices with  $Fe_3+$  and  $Ni_2+$ . In nanocrystalline samples asymmetry is in component due to confinement and length-distribution of nanoparticles. it is showed that shape of  $NiFe_2O_4$  is based upon on the synthesizing conditions [21].  $NiFe_2O_4$  may be characterised as a combination of normal and inverse spinel ferrite. With the in- crease of the calcination temperature or milling time the shape modifications from herbal everyday spinel form to combined spinel form and single great bands in the Ra- man spectra have grow to be asymmetric, with double peak like shape.

The Raman spectra of  $MnFe_2O_4$  nanocrystalline samples, obtained with the aid of using mechanochemical technique at low temperature, have not often visible doublet shape and it is able to be concluded that spinel shape of these samples is regularly normal.

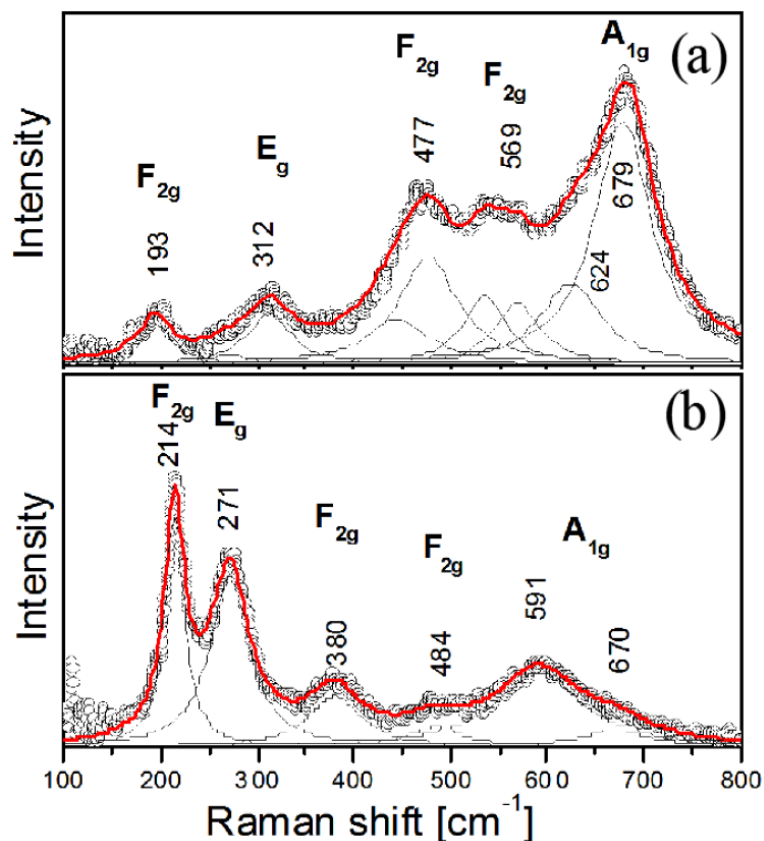


Fig. 2. Raman spectra at room temperature of the mixture of: (a)  $Ni(OH)_2$  and  $\alpha-Fe_2O_3$  and (b)  $Mn(OH)_2$  and  $\alpha-Fe_2O_3$  powders after 25 h milling time.

The Raman spectra of samples, received through blending of Ni(OH)<sub>2</sub> and  $\alpha$ -Fe<sub>2</sub>O<sub>3</sub> and (2) Mn(OH)<sub>2</sub> and  $\alpha$ -Fe<sub>2</sub>O<sub>3</sub> for 25 h are analyzed through the usage of deconvolution (Fig. 2) and modes are assigned, as usual. In the cubic ferrites, the modes at above six hundred cm<sup>-1</sup> regularly correspond to the motion of oxygen in tetrahedral AO<sub>4</sub> businesses, so the mode at 679 cm<sup>-1</sup> for NiFe<sub>2</sub>O<sub>4</sub> and doublet modes at 591 670 cm<sup>-1</sup> for MnFe<sub>2</sub>O<sub>4</sub> can be pretty considered as Ag symmetry. The other low frequency modes constitute the traits of the octahedral websites (BO<sub>6</sub>). The mode, discovered at spherical 679 cm<sup>-1</sup> for NiFe<sub>2</sub>O<sub>4</sub> and 591 670 cm<sup>-1</sup> for MnFe<sub>2</sub>O<sub>4</sub> may be assigned to tetrahedral Ni<sup>2+</sup> and Mn<sup>2+</sup> stretching, and band located at 477 cm<sup>-1</sup> and 484 cm<sup>-1</sup> entails the Fe<sup>3+</sup> vibration on the octahedral internet site in every instances. The 5 first-order Raman modes at approximately 193, 312, 477, 599 and 679 cm<sup>-1</sup> (Fig. 2a) and 214, 271, 380, 484 and 591 670 cm<sup>-1</sup> display off the large traits. The received 3 modes at approximately 193, 477 and 599 cm<sup>-1</sup> for NiFe<sub>2</sub>O<sub>4</sub> and 214, 380 and 484 cm<sup>-1</sup> for MnFe<sub>2</sub>O<sub>4</sub> belong to the symmetry type F<sub>2g</sub>. additionally, it is able to see that the modes 312 and 271 cm<sup>-1</sup> belong to identical symmetry E<sub>g</sub> for NiFe<sub>2</sub>O<sub>4</sub> and MnFe<sub>2</sub>O<sub>4</sub>, respectively. For in addition characterization of the synthesized NiFe<sub>2</sub>O<sub>4</sub> and MnFe<sub>2</sub>O<sub>4</sub> ferrites, IR spectra had been recorded withinside the variety of 57 hundred cm<sup>-1</sup> (Fig. 3). The maximum exaggerated capabilities in spectra, F<sub>1u</sub>(3) and F<sub>1u</sub>(4), correspond to the vibrations of positive ions in NiFe<sub>2</sub>O<sub>4</sub> and MnFe<sub>2</sub>O<sub>4</sub> in octahedral and tetrahedral sites, respectively. it's miles seemed that the higher band at 700 cm<sup>-1</sup> corresponds to the intrinsic vibrations of tetrahedral webweb page and the decrease band at four hundred cm<sup>-1</sup> is attributed to the vibrations of octahedral internet site online. The one of a kind values of the power feature for those modes are because of one of a kind values of metallic ion O<sup>2-</sup> distances for octahedral and tetrahedral sites. In reactivity spectra of NiFe<sub>2</sub>O<sub>4</sub> TO LO splitting of F<sub>1u</sub>(four) IR mode is visible.

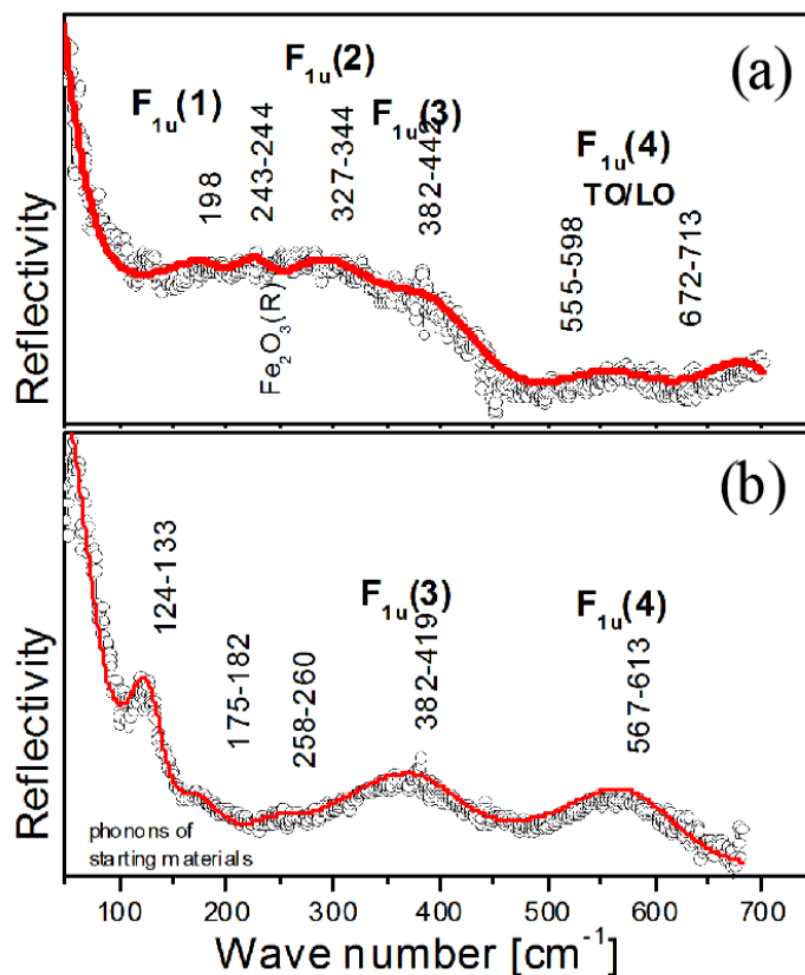


Fig. 3. IR spectra at room temperature of the mixture of: (a) Ni(OH)<sub>2</sub> and  $\alpha$ -Fe<sub>2</sub>O<sub>3</sub> and (b) Mn(OH)<sub>2</sub> and  $\alpha$ -Fe<sub>2</sub>O<sub>3</sub> powders after 25 h milling time

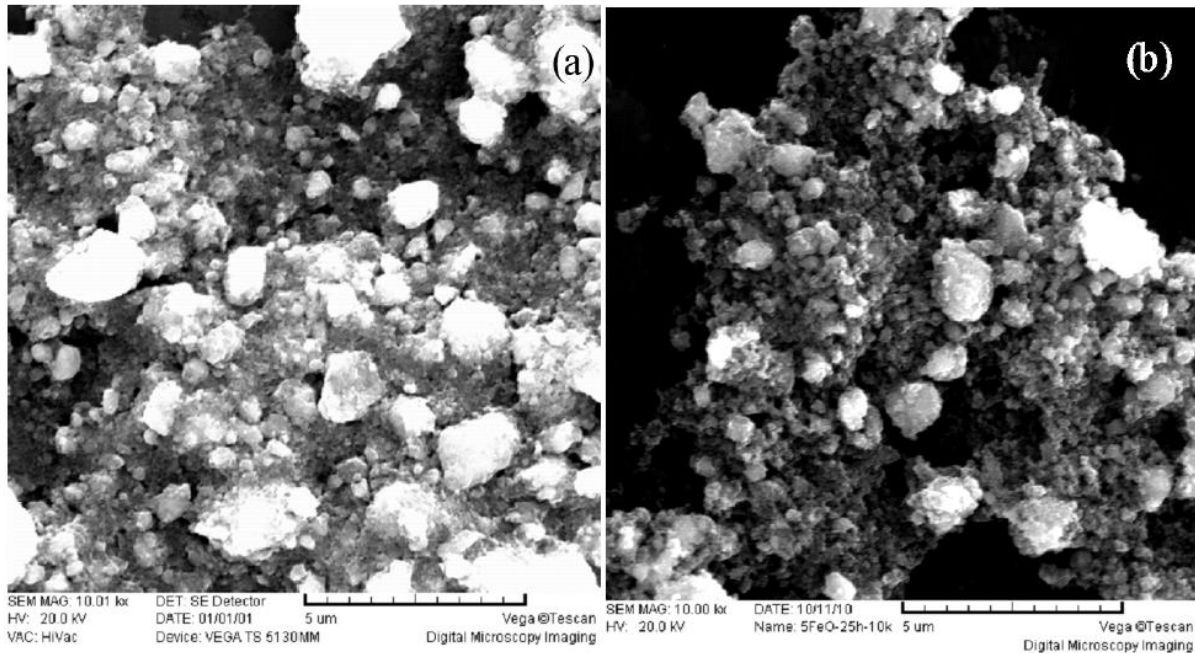


Fig. four. SEM pics of nanoscale of (a) NiFe<sub>2</sub>O<sub>4</sub> and (b) MnFe<sub>2</sub>O<sub>4</sub> powders after 25 h of milling time. Fig. four. SEM images of nanoscale of mechano synthesized (a) NiFe<sub>2</sub>O<sub>4</sub> and (b) MnFe<sub>2</sub>O<sub>4</sub> powders after 25 h of milling time.

discern four indicates the SEM micrographs for the pattern received from the aggregate of (1) Ni(OH)<sub>2</sub> and Fe<sub>2</sub>O<sub>3</sub> and (2) Mn(OH)<sub>2</sub> and Fe<sub>2</sub>O<sub>3</sub> powders through the easy mechanochemical synthesis after 25 h milling time, respectively. As end result of mechanochemical reaction, the powders emerge as a good buy and uniform in shape. at the same time as the beginning powder aggregate consisted predominantly of man or woman particles, the pattern of mechano-synthesized manganese ferrite includes aggregates of ne debris. The shape of the bulk of the crystallites regarded to be round. The ground morphology of the pattern as seen from the SEM consists of the grains, with relatively homogeneous grain distribution, with a mean grain length various from 1 to three μm.

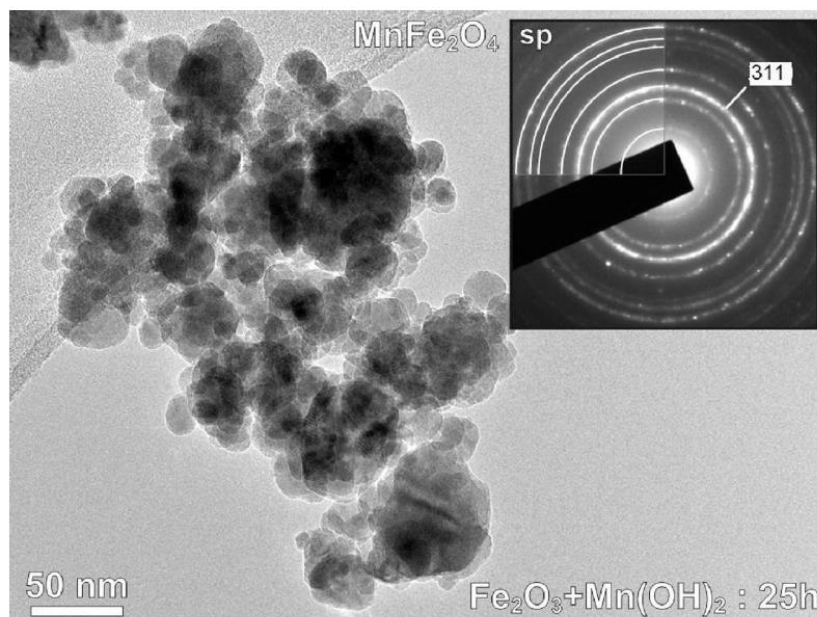


Fig. 5. TEM photograph with corresponding EDP of Mn(OH)<sub>2</sub> and α-Fe<sub>2</sub>O<sub>3</sub> after milling for 25 h. Spinel-kind reactions dominate the diffraction sample (inset).

The representative TEM photograph of the manganese ferrite particles is shown in Fig. 5. It suggests that the manganese ferrite particles obtained via this method are uniform in both morphology and crystallite length, however having agglomeration to some extent, because of the relative better interaction among magnetic particles. The manganese ferrite pattern received after 25 h of milling reveals the shape with crystallite sizes in the range of 10–50 nm. In addition, the electron diffraction pattern corresponding to the pattern acquired for 25 h of milling time is shown in Fig. 5 and may be nicely listed to (111), (220), (311), (400), (333), (440) and (533) of cubic spinel shape, that's consistent with the effects of XRD.

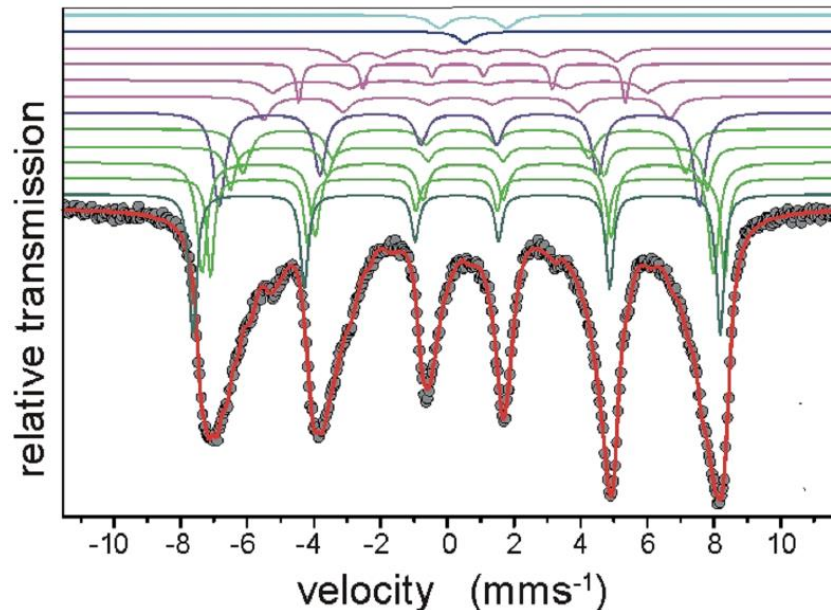


Fig. 6. Mossbauer spectra at room temperature of the mixture of  $\text{Mn}(\text{OH})_2$  and  $\alpha\text{-Fe}_2\text{O}_3$  powders after 25 h milling time.

Figure 6 suggests Mossbauer spectra for samples obtained at room temperature from the mixture of: (1)  $\text{Ni}(\text{OH})_2$  and  $\alpha\text{-Fe}_2\text{O}_3$  and (2)  $\text{Mn}(\text{OH})_2$  and  $\alpha\text{-Fe}_2\text{O}_3$  powders after 25 h milling time. The Mossbauer spectra for both samples encompass the twelve sub spectra. They're divided into three corporations, depending on the particles length. A huge nanoparticle calls for five sub spectra to explain cation distribution at the blended spinel  $(\text{Mn}_x\text{Fe}_{1-x})\text{T}(\text{Mn}_{1-x}\text{Fe}_{1+x})\text{MO}_4$ . The first sextet is assigned to ferric ion at tetrahedral website (T) with the cubic point symmetry institution  $T_d$ . It's confirmed with zero quadrupole splitting. Cations at this website sense the most powerful antiferromagnetic hyperfine interplay as result of the super exchange interplay through oxygen ions. The ferric ions positioned at octahedral coordination website (M) show four sextets because of different nearby surroundings. The ferric cations at (M) website online are very sensitive to the distribution of cations at (T) website online [17]. Therefore, the belonged sextets have broadened line widths. The octahedral website has the trigonal point symmetry  $D_{3d}$  organization, and one expects sure electric powered field gradient (EFG). The strength of hyperfine induction relies upon on the space among the magnetic ions and perspective of Fe–O–Fe bonds. Additionally, the strength decreases as the quantity of particles decreases.

The superparamagnetic rest effect takes place at very small nanoparticles and we can not take a look at a sextet any extra, as outcome. It's far located that the only doublet and the singlet are offered, originating from octahedral and tetrahedral coordination, respectively. The cation website online choice is affected whilst the dimensions of particles is small, too. We found out inside the first sample obtained from the aggregate of  $\text{Mn}(\text{OH})_2$  and  $\alpha\text{-Fe}_2\text{O}_3$  powders after 25 h milling time that amount of  $\text{Mn}^{2+}$  at tetrahedral site decreases from 76% to fifty one%, as length of particles decreased. The evaluation of the Mossbauer spectra of the investigated nanocrystalline ferrites acquired via mechanochemical remedy quantitatively confirm that  $\text{NiFe}_2\text{O}_4$  has an inverse spinel structure and  $\text{MnFe}_2\text{O}_4$  has mixed, often ordinary spinel structure.

### Conclusion

In this paper, we display that it is possible to reap NiFe<sub>2</sub>O<sub>4</sub> and MnFe<sub>2</sub>O<sub>4</sub> ferrites with the aid of smooth mechanochemical synthesis starting from the mixture of (1) Ni(OH)<sub>2</sub> and  $\alpha$ -Fe<sub>2</sub>O<sub>3</sub> and (2) Mn(OH)<sub>2</sub> and  $\alpha$ -Fe<sub>2</sub>O<sub>3</sub> powders. It has been shown that mechanochemical remedy of combinations with beginning substances ends in the amorphization of the starting powders, forming the section of Ni(OH)<sub>2</sub>, NiO, NiO(OH), FeO(OH) and Fe<sub>2</sub>O<sub>3</sub> after 4 h and 10 h of milling, and best NiFe O segment after 25 h, (case 1). Then again, looking at case (2), Mn(OH)<sub>2</sub> and Fe<sub>2</sub>O<sub>3</sub> stages arise after 3 h of milling, Fe<sub>2</sub>O<sub>3</sub>, MnO and FeO(OH) levels after 12 h and finally after 25 h only MnFe<sub>2</sub>O<sub>4</sub> section. On the premise of the Raman re- search there are found five first-order Raman lively modes. The intensity of the Raman and IR modes in the formation of NiFe<sub>2</sub>O<sub>4</sub> and MnFe<sub>2</sub>O<sub>4</sub> ferrite stages is alternatively low, as it is anticipated for nanocrystalline samples. The floor morphology of the samples includes the grains with pretty homogeneous distribution as seen from SEM. Crystallite size predicted from Scherrer's formulation is consistent with the consequences of TEM. The Mossbauer spectra show the only doublet and the singlet, originating from octahedral and tetrahedral coordination, respectively. The cation site online preference is affected when the size of particles are small, too. We observed out that quantity of Mn<sup>2+</sup> at tetrahedral site online decreases as length of particles decreased.

### Acknowledgments

This research changed into financially supported by using the Serbian Ministry of training and technology via tasks No. III45003 and 45015.

### References

- [1] S.S.P. Parkin, M. Hayashi, L. Thomas, *science* 320, 190 (2008).
- [2] S. Mornet, S. Vasseur, F. Grasset, P. Veverka, G. Goglio, A. Demourgues, J. Portier, E. Pollert, E. Dugust, *Prog. solid nation Chem.* 34, 237 (2006).
- [3] D.L. Zhao, X.W. Zeng, Q.S. Xia, J.T. Tang, *J. Alloys Comp.* 469, 215 (2009).
- [4] J.P. Fortin, F. Gazeau, C. Wilhelm, *Eur. Biophys. J.* 37, 223 (2008).
- [5] C.S. Gill, W. long, C.W. Jones, *Catal. Lett.* 131, 425 (2009).
- [6] V. epel k, I. Bergmann, A. Feldho , P. Heitjans, F. Krumeich, D. Menzel, F.J. Litterst, S.J. Campbell, k.D. Becker, *J. Phys. Chem. C* 111, 5026 (2007).
- [7] L. Wang, J. Ren, Y. Wang, X. Liu, Y. Wang, *J. Alloys Comp.* 490, 656 (2010).
- [8] A. Baykal, N. Kasapo lu, Y. ok seo lu, M.S. Toprak, H. Bayrakdar, *J. Alloys Comp.* 464, 514 (2008).
- [9] P. Osmokrovic, C. Jovalekic, D. Manojlovic, M.B. Pavlovic, *J. Opto. Adv. Mater.* 8, 312 (2006).
- [10] V. epel okay, M. Menzel, I. Bergman, M. Wiebcke, F. Krumeich, ok.D. Becker, *J. Magn. Magn. Mater.* 272, 1618 (2004).
- [11] J. Azadmanjiri, S.A. Seyyed Ebrahimi, H.okay. Salehani, *Ceram. Int.* 33, 1623 (2007).
- [12] R.V. Mangalaraja, S. Anathakmar, P. Monohar, F.D. Gnanam, M. Awana, *J. Mater. Sci. Eng. A* 367, 301 (2004).
- [13] M.A. Ahmed, E.H. El-Khawas, F.A. Radwan, *J. Mater. Sci.* 36, 5031 (2001).
- [14] M. Muroi, R. road, P.G. McCormick, J. Amighian, *Phys. Rev. B* 63, 184414 (2001).
- [15] F. Padella, C. Alvani, A. la Barbera, G. Ennas, R. Liberatore, F. Varsano, *Mater. Chem. Phys.* 90, 172 (2005).
- [16] E. Avvakumov, M. Senna, N. Kosova, *gentle Mechanochemical Synthesis: A basis for New Chemical technologies*, Kluwer instructional Publishers, Boston 2001.
- [17] M. Siddique, N.M. Butt, *Physica B* 405, 4211 (2010).
- [18] A.M. El Sayed, *Ceram. Int.* 28, 363 (2002).
- [19] Joint Committee on Powder Di raction standards (JCPDS) Powder Di raction file (PDF): International Centre for Di raction records: Newton rectangular, PA 2003.
- [20] Scherrer and Warren equations (B.E. Warren, X-ray Di raction, Addison Wesley, analyzing MA 1969).
- [21] A. Ahlawat, V.G. Sathe, V.R. Reddy, A. Gupta, *J. Magn. Magn. Mater.* 323, 2049 (2011)